



Characterization and control of a multi-primary LED light lab

MICHAEL J. MURDOCH*

Munsell Color Science Laboratory, Rochester Institute of Technology, 54 Lomb Memorial Drive,
Rochester, NY 14623, USA

*michael.murdoch@mail.rit.edu

Abstract: A new light lab facility has been commissioned at Rochester Institute of Technology with the research goal of studying human visual adaptation under temporally dynamic lighting. The lab uses five-channel LED luminaires with 16 bits of addressable depth per channel, addressed via DMX. Based on spectral measurements, a very accurate multi-primary additive color model has been built that can be used to provide “colorimetric plus” multi-primary channel intensity solutions optimized for spectral accuracy, color fidelity, color gamut, or other attributes. Several spectral tuning and multi-primary solutions are compared, for which accuracy results and IES TM-30-15 color rendition measures are shown.

© 2017 Optical Society of America

OCIS codes: (000.2170) Equipment and techniques; (230.3670) Light-emitting diodes; (330.1690) Color; (330.1710) Color, measurement; (330.1715) Color, rendering and metamerism; (330.7320) Vision adaptation.

References and links

1. M. J. Murdoch, M. G. M. Stokkermans, and M. Lambooij, “Towards perceptual accuracy in 3D visualizations of illuminated indoor environments,” *J. Solid State Lighting* **2**(1), 12 (2015).
2. C. Miller, Y. Ohno, W. Davis, Y. Zong, and K. Dowling, “NIST spectrally tunable lighting facility for color rendering and lighting experiments,” in *Proceedings of Light and Lighting Conference with Special Emphasis on LEDs and Solid State Lighting* (CIE, 2009), pp. 5–9.
3. IEC, Default RGB colour space – sRGB, International Standard IEC 61966-2-1 (IEC, 1999).
4. M. Fairchild and D. Wyble, “Colorimetric characterization of the Apple studio display (Flat panel LCD),” Munsell Color Science Laboratory Technical Report (1998).
5. M. J. Murdoch, M. E. Miller, and P. J. Kane, “Perfecting the color reproduction of RGBW OLED,” in *Proceedings of International Congress on Imaging Science 2006* (IS&T, 2006), pp. 448–451.
6. T. Ajito, K. Ohsawa, T. Obi, M. Yamaguchi, and N. Ohya, “Color Conversion Method for Multiprimary Display Using Matrix Switching,” *Opt. Rev.* **8**(3), 191–197 (2001).
7. H. Motomura, “Color conversion for a multi-primary display using linear interpolation on equi-luminance plane method (LIQUID),” *J. Soc. Inf. Disp.* **11**(2), 371–378 (2003).
8. A. Žukauskas, R. Vaicekauskas, P. Vitta, A. Tuzikas, A. Petrulis, and M. Shur, “Color rendition engine,” *Opt. Express* **20**(5), 5356–5367 (2012).
9. Y. Ohno, “Spectral design considerations for white LED color rendering,” *Opt. Eng.* **44**(11), 111302 (2005).
10. H. Ries, I. Leike, and J. Muschaweck, “Optimized additive mixing of colored light-emitting diode sources,” *Opt. Eng.* **43**(7), 1531–1536 (2004).
11. F. Zhang, H. Xu, and Z. Wang, “Optimizing spectral compositions of multichannel LED light sources by IES color fidelity index and luminous efficacy of radiation,” *Appl. Opt.* **56**(7), 1962–1971 (2017).
12. M. C. Chien and C. H. Tien, “Multispectral mixing scheme for LED clusters with extended operational temperature window,” *Opt. Express* **20**(Suppl 2), A245–A254 (2012).
13. N.-C. Hu, Y.-C. Feng, C. C. Wu, and S. L. Hsiao, “Optimal radiant flux selection for multi-channel light-emitting diodes for spectrum-tunable lighting,” *Light. Res. Technol.* **46**, 434–452 (2014).
14. S. Afshari, L. Moynihan, and S. Mishra, “An optimisation toolbox for multi-colour LED lighting,” *Light. Res. Technol.* **0**, 1–15 (2016).
15. Illuminating Engineering Society, IES Method for Evaluating Light Source Color Rendition. *IES TM-30-15* 2015; ISBN 978-0-87995-312-6
16. A. David, P. T. Fini, K. W. Houser, Y. Ohno, M. P. Royer, K. A. G. Smet, M. Wei, and L. Whitehead, “Development of the IES method for evaluating the color rendition of light sources,” *Opt. Express* **23**(12), 15888–15906 (2015).
17. International Commission on Illumination, “CIE 13.3-1995: Method of Measuring and Specifying Colour Rendering Properties of Light Sources.” (CIE, 1995).
18. Philips Lighting, SkyRibbon IntelliHue, <http://www.colorkinetics.com/Is/IntelliHue/skyribbon-wall-washing/>
19. ENTTEC, “DMX USB Pro Widget API Specification 1.44,” https://doi2kh495zr52.cloudfront.net/pdf/misc/dmx_usb_pro_api_spec.pdf

20. DMXKing, ultraDMX Micro, <https://dmxking.com/usbdmx/ultradmxmicro>
21. Photo Research, SpectraScan® Spectroradiometer PR-655,
<http://www.photoresearch.com/content/spectrascan%C2%AE-spectroradiometer>
22. MathWorks, MATLAB 2014b, https://www.mathworks.com/products/new_products/release2014b.html
23. International Commission on Illumination, “CIE 15: Colorimetry, 3ed” (CIE, 2004).

1. Introduction

Dynamic lighting is light that changes over time. Natural light is typically dynamic, including daylight’s diurnal variation in color and intensity, the effects of weather, and the variation seen in daylight filtered through trees or reflected from water. Artificial light is becoming ever more dynamic as digital addressable LED systems make changes in color and intensity easy and responsive. Already, dynamic lighting systems are being designed to influence circadian rhythms, to dim in response to occupancy or daylight entrance, to attract attention, and for specific tasks like focused reading or calming effects. Programming these new dynamic lighting systems mostly falls to lighting designers or product managers, who rely on their experience and limited market research. With the exception of nonvisual, circadian effects, there is not much scientific research on the human visual system’s capability for adaptation under dynamic lighting. It is exactly this field of research for which the Dynamic Visual Adaptation Lab (DVA Lab) was recently commissioned in RIT’s Munsell Color Science Laboratory (MSCL). Describing the DVA Lab’s design and performance builds on several different background areas, including illuminators and light labs, additive color system modeling, and multispectral control algorithms.

Color scientists, graphic artists, and others have long relied on viewing booths, daylight simulators, and other illuminators to provide standard illumination for visual tasks. Recent LED-based viewing booths provide stable illumination, typically manually switchable between a variety of spectral power distributions. Room-scale illumination systems or light labs have been built for research purposes, including at Philips Research [1] and at NIST [2]. The Philips lab was primarily used for the assessment of perceived atmosphere in static scenes. The NIST facility was designed for spectral tuning, meaning a wide range of spectral power distributions enabled by a large number (22) of LED spectral channels. Some recent commercial viewing booths and illuminators have begun to offer spectral tuning capability. The DVA Lab was intended primarily for careful temporal control and secondarily for spectral tuning, at least in terms of overall object color saturation. Preference was given for commercial light fixtures for reasons of robustness and a standard control interface.

Creating a desired light output with an illumination system, be it a colorimetric specification or a spectral match, requires an invertible model of the system’s behavior. Recognizing the similarity between multi-channel (or multi-LED) lighting systems and multi-primary displays, a starting point is the colorimetric model often employed in 3-primary (RGB) display systems, with an accounting for a system nonlinearity and a matrix representing the linear combination of basis primaries that are assumed to be independent and colorimetrically stable. The structure of this model is the basis of standard RGB encodings like sRGB [3], and can be used to model most display systems [4]. Importantly, a 3x3 matrix is invertible, meaning it is possible to directly and unambiguously compute required *RGB* values from desired *XYZ* colorimetry. Setting the nonlinearity aside, the forward additive colorimetric model is:

$$\begin{bmatrix} X \\ Y \\ Z \end{bmatrix}_{est} = \begin{bmatrix} X_R & X_G & X_B \\ Y_R & Y_G & Y_B \\ Z_R & Z_G & Z_B \end{bmatrix} \begin{bmatrix} R \\ G \\ B \end{bmatrix} + \begin{bmatrix} X \\ Y \\ Z \end{bmatrix}_{flare} \quad (1)$$

Where the vector XYZ_{est} represents the estimated *XYZ* tristimulus values for a given input vector *RGB*, which comprises the primaries’ relative intensity values, each of which lies in the closed interval [0, 1]. The 3x3 primary matrix contains the *XYZ* colorimetry of the three

color primaries, and the vector XYZ_{flare} is an offset to account for non-zero light output when the RGB intensities are set to zero (this is generally needed for displays, but less likely for lighting systems unless there is ambient light). This model is essentially a linear combination of the primaries' colorimetry.

The matrix-based additive system model can be extended to any number of primaries, but of course in so doing, colorimetric invertibility is lost, meaning there are multiple primary intensity solutions for a specified XYZ . Primaries beyond three correspond to additional degrees of freedom, so a multi-primary solution requires additional constraints beyond colorimetric matching; such a solution may be either direct or iterative. Examples of direct computations include a red, green, blue, and white (RGBW) OLED solution that directly computes the most power efficient solution by white replacement [5], a multi-primary display algorithm that selects among multiple matrix solutions [6], and a "virtual primary" solution that reduces the problem to an invertible 3-primary system [7]. A lighting-specific example using red, green, blue, and amber (RGBA) LEDs uses weighted combinations of colorimetric RGB and AGB solutions to modulate the perceived color rendition characteristics [8]. Iterative multi-primary solutions, discussed below, typically rely on nonlinear optimization techniques.

It is important to realize that the colorimetric matrix model is an integrated representation of an underlying spectral matrix model, in which the primaries' XYZ tristimulus values are replaced by their spectral power distributions. This model goes a step beyond metameric solutions (XYZ matches), and allows consideration of spectral solutions. For example, a forward additive spectral model (with m spectral bands) for n primaries is given in Eq. (2). The vector $S(\lambda)_{est}$, the estimated spectral power distribution over spectral bands λ , is a linear combination of the primaries' spectral power distributions $S(\lambda)_j$, weighted by the primary intensities P_j and, if necessary, an additive offset to account for flare:

$$\begin{bmatrix} S(\lambda_1) \\ \vdots \\ S(\lambda_m) \end{bmatrix}_{est} = \begin{bmatrix} S(\lambda_1)_1 & \cdots & S(\lambda_1)_n \\ \vdots & \ddots & \vdots \\ S(\lambda_m)_1 & \cdots & S(\lambda_m)_n \end{bmatrix} \begin{bmatrix} P_1 \\ \vdots \\ P_n \end{bmatrix} + \begin{bmatrix} S(\lambda_1) \\ \vdots \\ S(\lambda_m) \end{bmatrix}_{flare} \quad (2)$$

which may be equivalently expressed (and is seen in other literature) as:

$$S(\lambda)_{est} = \sum_{i=1}^n p_i S(\lambda)_i + S(\lambda)_{flare} \quad (3)$$

An unconstrained inversion of this model, such as a [non-negative] pseudo-inverse, results in a least-squares spectral match, and thus not necessarily – *and not likely* – a colorimetric match. Well-chosen constraints can take advantage of the available degrees of freedom in smarter ways.

Much literature has addressed the need for constrained optimized inversions. Some work on this topic has focused on selecting LEDs for illumination system design, rather than the range of solutions possible in a multi-primary LED system, but the objectives are often the same. Linear and nonlinear approaches were proposed that maximize efficacy and/or color rendering characteristics [9–11]. Similarly, though additionally modeling the current and temperature dependence of LEDs, efficacy and light quality were maximized for given colorimetric goals [12]. As multi-primary systems became more common, researchers addressed solutions such as matching standard illuminants. A general solution applied to a 12-LED multi-primary system was used to compute max-flux solutions with colorimetric values matching several standard illuminants [13]. Bringing together many aspects of these research approaches, a computational toolbox was described that allows multi-primary optimizations with different constraints [14].

Color rendition of light sources is a common thread in many of these papers, and it is one of the most important performance characteristics of lighting systems. For the sake of the

present document, however, only the basic color rendition scores defined by IES TM-30-15 (TM-30) [15] are discussed. As explained in [16], TM-30 was designed to supersede and improve the legacy CIE General Color Rendering Index (CRI) [17] with a combination of summary scores and plotted graphics. TM-30 defines the computation of two measures that compare the color rendition of a given test light source to that of a standard illuminant selected to match its correlated color temperature (CCT). TM-30 R_f , or fidelity, is an average of color similarity between objects under the test and reference light sources, and R_g , or gamut, is an average relative color saturation of objects under the test and reference light sources. Condensing the generally-complex characteristics of color rendition to a two-measure plane provides a useful, but very simplified summary, so TM-30 also provides hue-dependent R_f and R_g bar charts, along with diagrams of hue and chroma distortion characteristics. One detail to point out is that typical light sources, with fixed chromaticity and spectral characteristics, typically plot as a point in TM-30 (R_f , R_g) space; however, multi-primary, spectrally-tunable, color-changing light sources can plot as a set of points or a locus in this space, depending on how they are driven, as will be shown later in this paper. Color rendition is an important characteristic that can be an objective of “colorimetric plus” multi-primary control solutions, solving the inversion of Eq. (2), that are relevant for the DVA Lab.

2. DVA lab & lighting design

The DVA Lab was built in a 3.66 x 4.27 m room in the Munsell Color Science Laboratory at RIT. One of the long walls is made up of three sliding wooden panels that form a moveable wall, which can be opened 2.4 m wide. On the 2.44 m high ceiling, 14 Philips SkyRibbon IntelliHue Wall-Washing fixtures [18], which are 5-primary (Red, Green, Blue, Mint Green, White: RGBMW) LED luminaires, are arranged in a rectangle 60 cm from the walls. The intention was to create a space with smooth vertical luminance, accepting some natural non-uniformity as more ecologically valid than a ganzfeld for testing visual adaptation to lighting in real architectural spaces. The light-to-dark gradient in illumination is approximately 3:1. Pictured in Fig. 1, the DVA Lab was finished with white ceiling grid and tiles, walls painted with a matte white paint with an average reflectance of 93%, and floor carpeted in variegated gray with average reflectance of 7%.

The LED fixtures are controlled via DMX, a digital protocol originally designed for theatre lighting control, which allows data transfer at 40 Hz of one-byte intensity values to up to 512 logical addresses. The 14 SkyRibbon fixtures are each made up of two addressable 30 cm sections, each of which has 5 channels (RGBMW), each of which is controllable at 16-bit depth by using two DMX bytes; these total 280 DMX addresses. The system can be driven either by a programmable Philips controller or, for easier integration with custom software used for psychophysical testing, using the ENTTEC DMX-USB API [19] on a computer via a USB-to-DMX interface such as the DMXKing ultraDMX Micro [20]. The latter control was used for all the measurements described herein.



Fig. 1. Photograph of the 3.66 x 4.27 m DVA Lab with rear wall illuminated by a spatial gradient from cool white 9000K to warm white 2000K.

3. LED system measurement & modeling

Comprehensive spectral measurements were made of the DVA Lab's LED system. Because the lab is designed for visual adaptation, we are more interested in the radiance of the walls, which will fill an observer's field of view during experiments, than of the irradiance onto lab surfaces. Thus, tele-spectroradiometric measurements were made of the brightest part of the rear wall, e.g. in Fig. 1 approximately $\frac{1}{4}$ of the way from the ceiling to the floor, above the round wall-cover and under the center of one of the LED luminaires. Unlike in the photo in Fig. 1, measurements were made with all luminaires set to the same color, so the entire lab was uniformly colored. A Photo Research PR-655 spectroradiometer with 8 nm spectral bandwidth [21] was interfaced to a PC running MATLAB 2014b [22] for scripted measurements. Spectral data from 380 to 780 nm at 4 nm spacing was collected, and converted to colorimetric values using the CIE 1964 10-degree standard observer [23].

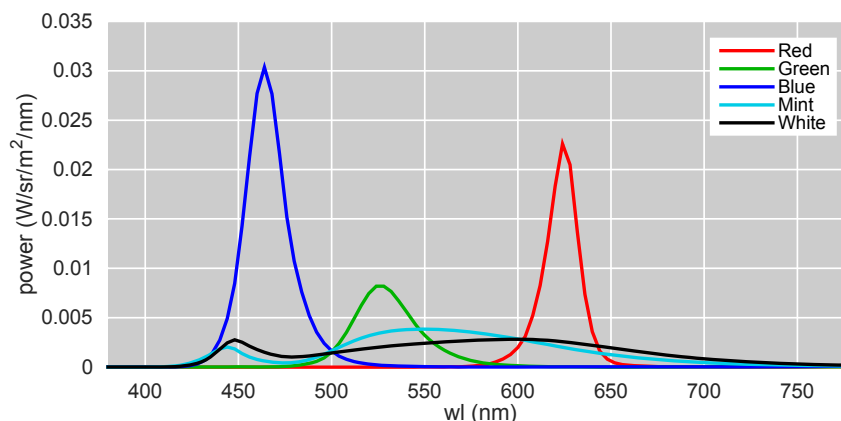


Fig. 2. SPDs of maximum output of the 5 LED primaries.

The characteristic spectral power distributions (SPDs) of each LED channel are shown in Fig. 2. The *RGB* SPDs are relatively narrow-band discrete LEDs, while the *M* and *W* SPDs

are characteristic of phosphor-converted LEDs with a small blue-pump peak around 450 nm and a broadband phosphor emission, peaking about 550 nm for M and about 600 nm for W . With all five channels at maximum intensity, the measured luminance of the wall is 837 cd/m². Each LED channel was measured at 61 different intensity levels, repeated 8 times, and the spectral shape is remarkably consistent due to the PWM drive. This consistency satisfies one of the requirements for a matrix-based additive color model, colorimetric stability, meaning the chromaticities of the primaries do not vary with intensity.

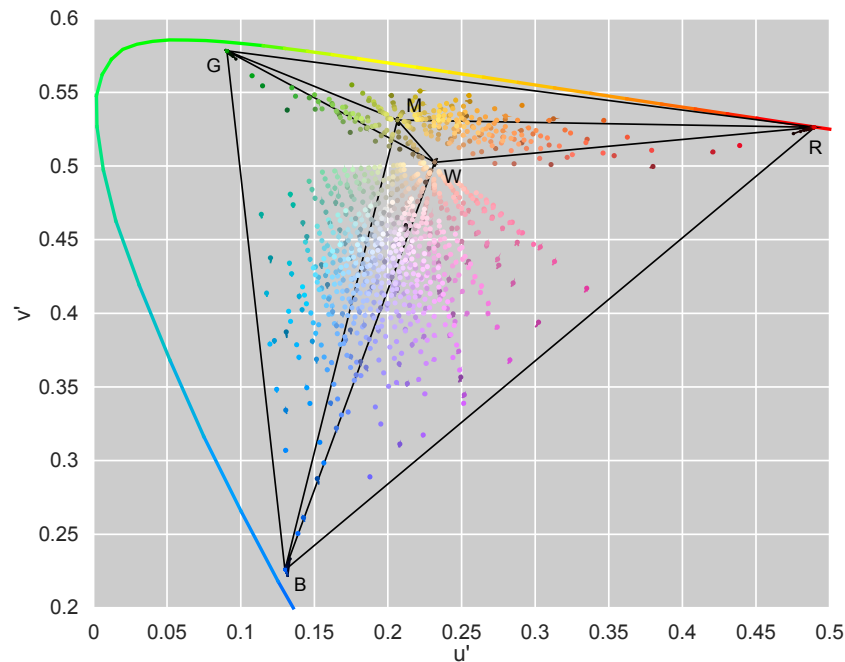


Fig. 3. 1964 $u'v'$ UCS plot of the 5 primaries (labeled vertices of the black polygons) and the 1,024 colors measured to verify the additive system model (colored dots). The colored curve represents the spectral locus, the physical boundary of monochromatic light.

Plotted in 1964 $u'v'$ chromaticity coordinates in Fig. 3, the five color primaries are shown as the vertices of the black polygons. The RGB primaries define the outer boundaries of the chromaticity gamut, and the M and W primaries plot within it. The W primary lies near a 4000 K CCT white, and the M is slightly yellow-green of it. Also shown in the chromaticity diagram are the 1,024 colors used to verify the additive color model, described below. The LED system also satisfied the second requirement for the additive color model, channel independence, meaning the intensity of a given LED channel is not affected by the intensity of any other channel. This was tested by comparing the sum of channels' separately-measured XYZ_{10} values with measured XYZ_{10} of all five channels on simultaneously, and the absolute difference was less than 0.25% for all intensity levels.

With these requirements met, the LED system was modeled as described above as a spectral additive color model using a 101 x 5 matrix (101 spectral bands by 5 primary channels) in the form of Eq. (2) – the matrix is comprised of the SPDs plotted in Fig. 2 – and as a corresponding colorimetric model with a 3 x 5 primary matrix of measured maximum XYZ_{10} of the primaries (with Y in units of cd/m²) is shown in Eq. (4):

$$\begin{bmatrix} X \\ Y \\ Z \end{bmatrix}_{est} = \begin{bmatrix} 265 & 67.8 & 135 & 203 & 188 \\ 127 & 192 & 104 & 232 & 182 \\ 0.273 & 13.7 & 820 & 82.9 & 113 \end{bmatrix} \begin{bmatrix} R \\ G \\ B \\ M \\ W \end{bmatrix} \quad (4)$$

Flare for the system (meaning dark-room luminance) was essentially zero, so that term of the model was not used. The nonlinearity of the LED system was measured using the ramps mentioned. Look-up tables (LUTs) were computed to relate 16-bit digital drive value to intensity (fraction of the maximum luminance) for each primary channel.

One negative performance attribute was observed: thermal droop, the well-known LED drop in efficiency and output as they warm up. The LED luminaires do not actively control their temperature, so droop of up to 6% loss in luminance was observed over a time period of about an hour. Accounting for this directly is not trivial, as it would involve either modeling the thermal behavior and keeping track of the recent history of each LED or a closed-loop control strategy. The present tactic is to simply warm up the LEDs by setting all channels to about 60% intensity for an hour. All measurements and verifications were made in repeated sets over the course of about a week, each set after one-hour warm-up periods.

Verifying the accuracy of the spectral additive system model consisted of comparing actual measured spectra with model-estimated spectra, for a set of verification colors. In the 5-D input primary intensity space, a 4-level grid was created of 5^4 or 1,024 colors. Two sets of measured and estimated spectra were converted to XYZ , u^*v^* , and CIELAB using a reference white of the chromaticity coordinates of the W primary (4000K CCT) at the luminance of the all-channel maximum. The differences, in Table 1, were quite small; notably, the maximum error in CIEDE2000 (ΔE_{00}) [23] was less than 1, with a mean of 0.26; and, the mean luminance error was 0.51 cd/m^2 , compared to the average luminance over all measured verification colors of 338 cd/m^2 and maximum system luminance of 837 cd/m^2 . Qualitatively speaking, these are quite small errors; the largest of these small errors were mostly found in darker colors with v^* less than 0.45 – barely visible in Fig. 3, which plots the expected colors as dots connected to measured colors by thin lines.

Table 1. Mean, median, and max model errors were computed over 1,024 verification colors, each measured twice. Luminance Y values are in units of cd/m^2 , and the average measured luminance of the verification colors was 338 cd/m^2 .

| | ΔE_{00} | Δu^*v^* | $\Delta Y (\text{cd/m}^2)$ |
|---------------|-----------------|-----------------|----------------------------|
| Mean | 0.26 | 0.00079 | 0.51 |
| Median | 0.22 | 0.00074 | 0.44 |
| Max | 0.94 | 0.0036 | 2.9 |

4. LED multi-primary solutions

Several multi-primary channel intensity solutions were implemented for comparison. A set of 101 equi-luminant (175 cd/m^2) colors, from 2000K to 9000K, were selected as target spectral power distributions. In the same way that TM-30 defines reference colors, spectra at the warm end of the set are Planckian blackbody radiators, at the cool end are daylight sources, and between 4000K and 5000K are defined by a smooth linear transition between. The u^*v^* and XYZ colorimetric values of these target SPDs are shown in Fig. 4; note the slight wiggle in the path in u^*v^* due to the transition between the Planckian and daylight spectral loci. In the following section, examples of different spectral tuning variations for reproducing these target SPDs are explained.

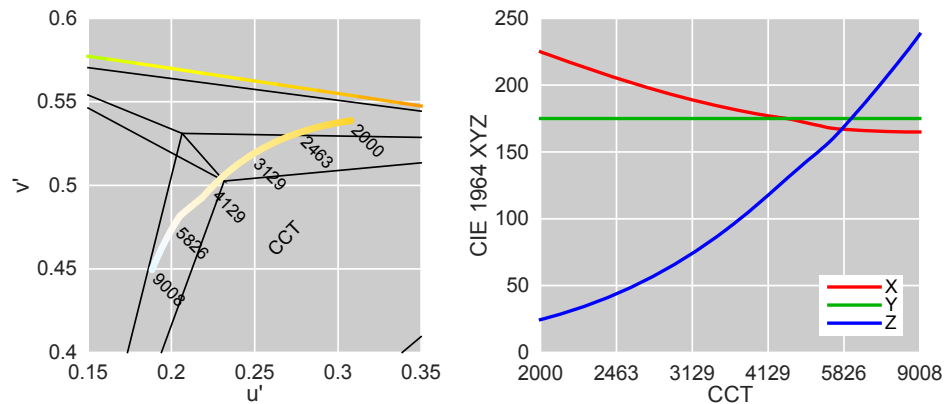


Fig. 4. At left, the $u'v'$ chromaticity values of 101 target colors from 2000K to 9000K, labeled, and plotted in approximate color. The black polygons are the same as plotted in Fig. 3. At right, the XYZ tristimulus values of these colors (showing constant luminance of 175 cd/m^2), plotted versus CCT. The 101 target colors are spaced evenly in the more perceptually-uniform $u'v'$ space, thus the unintuitive spacing of the CCT axis labels.

Colorimetric RGB and RGBW

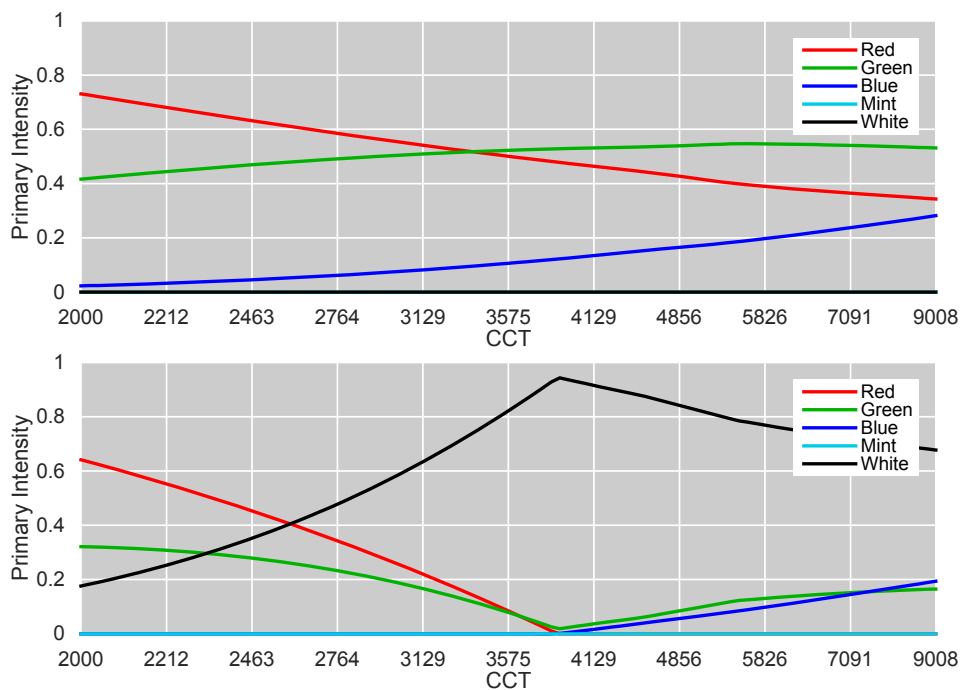


Fig. 5. Plots of primary intensity versus CCT for an RGB-only colorimetric solution (top) and for an RGBW solution using maximum W replacement (bottom).

A 3-primary additive color system has an unambiguous solution for any colorimetric target within its gamut. Using only the RGB LEDs, thus setting the M and W primary intensities to zero, Eq. (4) simplifies to a 3×3 matrix model that can be solved by matrix inversion. RGB solutions for each of the XYZ target colors shown in Fig. 4 were computed in this way, and are shown in the upper frame of Fig. 5, plotted versus CCT.

As is expected, the amount of R decreases from warmer, low-CCT to cooler, high-CCT colors, and the amount of B increases over the same range. In the lower frame of Fig. 5 is an RGBW solution, computed via white replacement (utilizing as much W primary as possible in place of a metameric combination of RGB , as explained in [5]). The RGBW solutions still has more R at the low-CCT end, and more B at the high-CCT end, but R , G , and B all go to nearly zero around a CCT of 4000K, replaced nearly entirely by the W primary, which on its own produces 4000K white light. Both the RGB and RGBW solutions provide colorimetric matches to the target colors.

Colorimetric plus spectral match and max- R_f

An obvious objective for spectral tuning is a spectral match. With only 5 LED channels, there is not enough spectral variation to make excellent spectral matches, but indeed for any given target SPD, the spectral error can be minimized with a least-squares fitting algorithm. However, for the purposes of the DVA Lab, accurate color is critical: thus, the idea of “colorimetric plus” solutions, meaning that the optimization must be constrained to solutions that firstly are colorimetric matches to the target, and secondarily minimize an objective function, such as spectral error. MATLAB provides such a constrained optimization with the function *fmincon*, which allows a linear constraint, essentially the no-flare version of Eq. (1). Comparing the spectral match solutions with the RGB-only solutions, Fig. 6 shows the aim SPD and two solution SPDs at three example CCT values. This illustrates that the spectral match is a better match than the RGB solution to the aim SPD, but still not excellent.

The colorimetric-plus spectral match solutions for all 101 target SPDs in the 2000 – 9000K CCT range are shown in the upper frame of Fig. 7. Spectral minimization favors the broader SPDs of the M and W primaries over RGB , but of course the R and B with some G are necessary at the extreme CCT values. Apparently, M with R makes a better spectral match to lower-CCT Planckian SPDs, and W with B improves the spectral match for higher-CCT daylight SPDs.

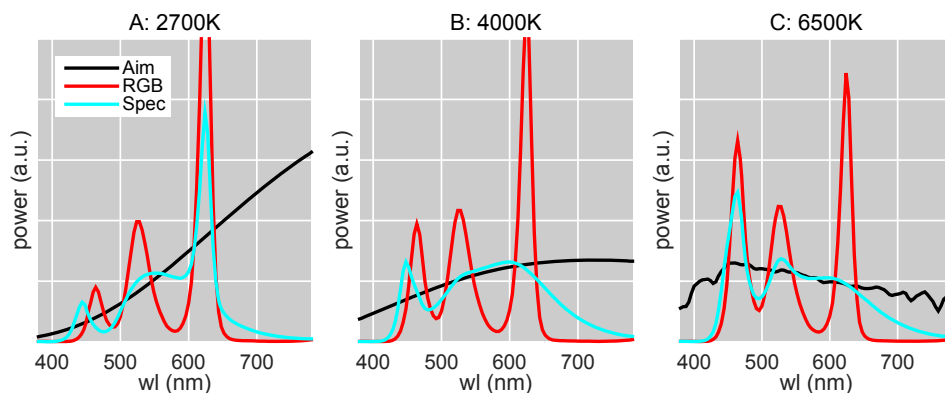


Fig. 6. Three panels show the aim SPD (black) with the RGB-only solution SPD (red) and the spectral-match SPD (cyan) for three example CCTs: 2700K (A), 4000K (B), and 6500K (C).

Another example of spectral tuning is to affect the color rendition of the light source, for example by maximizing TM-30 R_f . Again, this is a “colorimetric plus” constrained optimization, which is highly nonlinear thanks to the complexity of the TM-30 computation, but is still possible with MATLAB’s *fmincon* function. Colorimetric plus max- R_f solutions for the target SPDs are plotted in the lower frame of Fig. 7. The similarity between it and the spectral match should not be a surprise, because a perfect spectral match to a Planckian or daylight SPD would by definition score a maximum R_f value of 100. It is only because the spectral matches are not excellent that a slightly different weighting of primary intensities can

maximize the R_f score beyond that of the spectral match. A few wiggles in the plotted intensity versus CCT can be seen (especially in the W near 5000K, where the balance between W and M appears slightly unstable); this is due to the minimization of each target CCT being independent from all others, and hints that a secondary smoothness constraint might be useful.

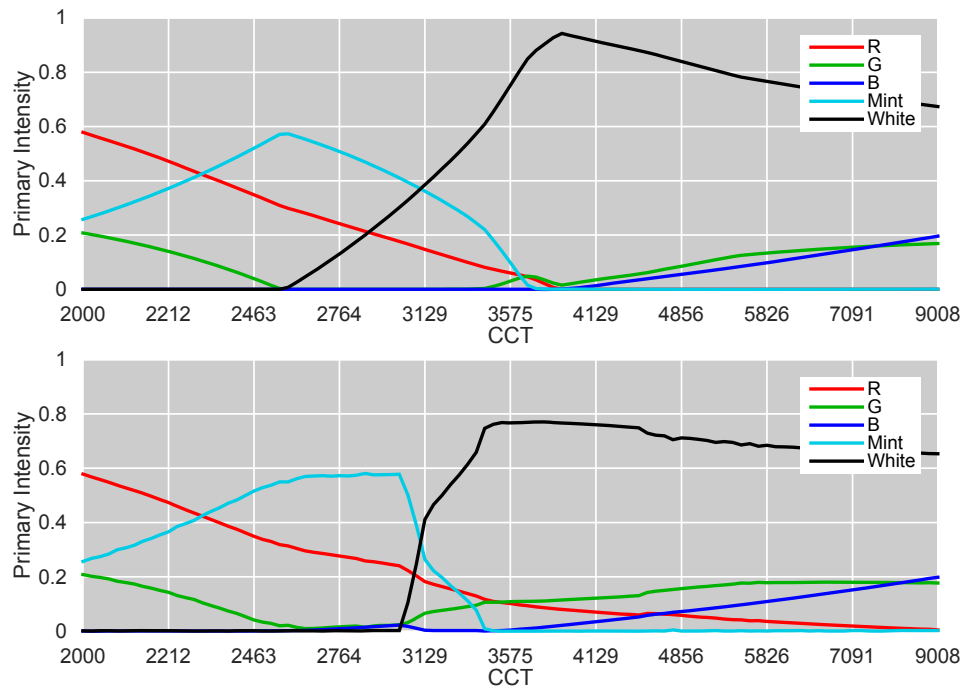


Fig. 7. Spectral Match and Max- R_f . Plots of primary intensity versus CCT for a colorimetric plus spectral match (top) and for a colorimetric plus max- R_f solution (bottom).

Colorimetric accuracy

The above plots show the LED channel drive values that are modeled to match the target CCT colorimetric and spectral values. They were tested in the DVA Lab to see how closely they came to their targets, measured with the PR-655 as described previously, but several months later. The average errors over the 101 target CCT colors in CIE u^*v^* are listed in Table 2. Overall the numbers are small, but it is worth noting that the error levels are about three times higher for target CCT solutions in which RGB are used heavily than for solutions in which M and W are used. Mean errors for the spectral match and max- R_f solutions of less than 0.001 in delta u^*v^* are very good and expected to be below the threshold for visibility.

Table 2. Mean, median, and max errors in Delta u^*v^* were computed over 101 target CCT colors ranging from 2000 to 9000 K for each of the multi-primary solutions, in columns.

| | RGB-Only | RGBW | Spectral Match | Max- R_f |
|---------------|----------|--------|----------------|------------|
| Mean | 0.0034 | 0.0020 | 0.00082 | 0.00090 |
| Median | 0.0034 | 0.0014 | 0.00037 | 0.00053 |
| Max | 0.0038 | 0.0036 | 0.0017 | 0.0021 |

Differences in color rendition

Each of the above multi-primary solutions produce colorimetric matches, but they have different SPDs, which means they may render object colors differently. White RGB LEDs typically have low-fidelity, high-gamut color rendition characteristics, while white phosphor-converted LEDs typically have higher fidelity, moderate-gamut characteristics. Each multi-primary solution uses the primaries differently, and for all solutions, over the set of target CCT colors, the changing blends of LED primaries means that the color rendition characteristics are not constant. Recognizing that TM-30 (R_f , R_g) plots do not tell a complete story, it is nonetheless instructive to compare the results of the different multi-primary solutions.

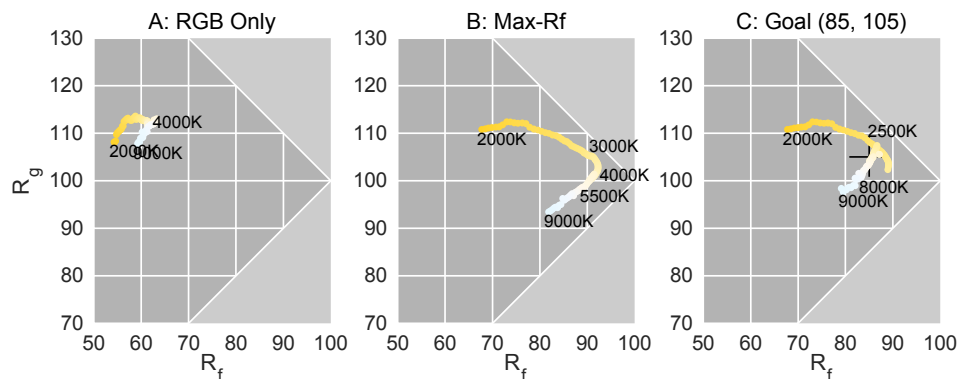


Fig. 8. Each plot shows the TM-30 (R_f , R_g) values of the 101 test colors over the CCT range, where R_f , or fidelity, indicates how similarly, on average, a light source renders object colors relative to a reference source; and R_g , or gamut, indicates the average chroma of rendered object colors relative to the reference. The point (100, 100) corresponds to a perfect match in color rendition to the reference. Plot A shows the colorimetric RGB-only solution, B shows the colorimetric plus Max- R_f solution, and C shows the colorimetric plus goal of (85, 105).

In Fig. 8, plot A shows the (R_f , R_g) scores of the colorimetric RGB solution, which wander slightly in the neighborhood of (60, 110). Plot B shows the colorimetric plus max- R_f solution – here it is clear that R_f is highly dependent on CCT. At all CCTs, this solution is higher in R_f than the RGB only solution, but R_f varies from about 68 to 92, while at the same time going from R_g 112 to 92. Such a variation in color rendition, even if incompletely described by the averaging that results in these plots, might be distracting in a visual adaptation experiment that involves any colored objects. For this reason, another colorimetric plus solution was computed with an optimization function the distance in TM-30 (R_f , R_g) space to a goal of (85, 105), a point chosen because it is achievable for most CCTs, even if it has lower R_f than the system can reach for some CCTs. The result is in Plot C, which shows that while the lower- R_f 2000K persists, points in the CCT range from about 2500 to 8000K remain within about 5 units of the goal. This level of spectral tuning, where an excellent spectral match remains difficult, but important color rendition characteristics can be controlled, on average, is very valuable for the DVA Lab and for LED systems with a few (approx. 4-8) spectral channels.

Future work

One topic of interest is to generalize the above results to non-white colors. The target colors described herein are all along the Planckian and daylight loci, meaning they are all perceptually whitish, ranging from warm white to cool white. Target SPDs are clearly defined, and TM-30 measures of color rendition are all valid. However, for non-white colors, CCT is undefined, target SPDs may not exist, and there are no measures for color rendition (TM-30 is explicitly not defined for non-white colors). Yet, many non-white colors remain

interesting for adaptation research, not to mention for application in architectural lighting. A measure for color fidelity for non-white colors would be extremely valuable; until it exists, a rule-of-thumb approach of a colorimetric plus solution that also constrains the SPD to minimize local slope will be used.

As mentioned, a main objective of the DVA Lab is the study of dynamic lighting, thus accurate temporal control is very important. The measurements included in this paper were all conducted with static light settings, which excepting thermal droop effects are not expected to be different for dynamic lighting. Visually, temporal transitions made with the target CCT colors described appear very smooth. However, we do not yet have measurements of dynamic stimuli that objectively confirm there are no flicker or transient color or luminance errors.

One possibility for future development is closed-loop control; a faster spectrometer than the PR-655 used for these measurements would allow rapid response to color errors, for example caused by thermal droop. The use of a control loop would have to be balanced with the need for dynamic lighting settings, so it would have to be fast and smooth in its effect. Literature includes control loops, but they generally take seconds to stabilize [2], much too slow for the experiments desired for the DVA Lab.

A final implementation detail is worth mentioning, related to the optimizations used to generate some of the colorimetric plus solutions. Optimizations need only be performed once for a given target color, and saved for later use. A 3D-to-5D LUT, that for example stored the 5-primary intensity required for given XYZ target input, for a given colorimetric plus solution strategy, would be one flexible, practical implementation. For some tasks, like a CCT series, simply storing the 101 5-primary intensities calculated above would be sufficient for later playback in the lab.

5. Conclusion

The performance of the newly-constructed Dynamic Visual Adaptation Lab, in terms of colorimetric accuracy and spectral tuning for lighting characteristics, has been confirmed. The lab is designed for controlled visual experiments studying dynamic visual adaptation, meaning chromatic and luminance adaptation while the lighting changes over time.

The lab contains 14 5-channel LED fixtures controlled via DMX, which have been comprehensively measured and modeled. The overall accuracy of the LED additive system model is about 0.25 Delta E_{00} for the entire color gamut, or about 0.0007 Delta $u'v'$, which is excellent for visual adaptation research. The LED additive system model is represented in both colorimetric matrix terms, similar to a display model, and in spectral terms, allowing inverse solutions via matrix and via nonlinear optimizations. Using “colorimetric plus” multi-primary solutions, in which a first constraint of colorimetric accuracy is met, and a second objective function minimization leads to a primary intensity solution for a given target color, shows success and flexibility.

Multi-primary solutions using RGB-only and RGBW colorimetric solutions have been shown, along with colorimetric plus solutions including spectral match, max- R_f , and an (R_f , R_g) goal, using TM-30 measures of color rendition. It is useful to plot loci of color transitions in TM-30 (R_f , R_g) space. Future work will include variations on these multi-primary solutions as well as temporal smoothness constraints. Psychophysical experiments to measure dynamic visual adaptation and temporal color perception will commence imminently.

Acknowledgments

The author would like to thank Philips Color Kinetics for generously providing the Philips SkyRibbon LED luminaires and drivers to RIT.